J Neurophysiol 121: 1501–1512, 2019.
First published February 20, 2019; doi:10.1152/jn.00748.2018.

RESEARCH ARTICLE | *Sensory Processing*

Processing of fast amplitude modulations in bat auditory cortex matches communication call-specific sound features

Stephen Gareth Hörpel and Uwe Firzlaff
Chair of Zoology, Department of Animal Sciences, Technical University of Munich, Freising, Germany

Submitted 2 November 2018; accepted in final form 15 February 2019

Hörpel SG, Firzlaff U. Processing of fast amplitude modulations in bat auditory cortex matches communication call-specific sound features. *J Neurophysiol* 121: 1501–1512, 2019. First published February 20, 2019; doi:10.1152/jn.00748.2018.—Bats use a large repertoire of calls for social communication. In the bat *Phyllostomus discolor*, social communication calls are often characterized by sinusoidal amplitude and frequency modulations with modulation frequencies in the range of 100–130 Hz. However, peaks in mammalian auditory cortical modulation transfer functions are typically limited to modulation frequencies below 100 Hz. We investigated the coding of sinusoidally amplitude modulated sounds in auditory cortical neurons in *P. discolor* by constructing rate and temporal modulation transfer functions. Neuronal responses to playbacks of various communication calls were additionally recorded and compared with the neurons' responses to sinusoidally amplitude-modulated sounds. Cortical neurons in the posterior dorsal field of the auditory cortex were tuned to unusually high modulation frequencies: rate modulation transfer functions often peaked around 130 Hz (median: 87 Hz), and the median of the highest modulation frequency that evoked significant phase-locking was also 130 Hz. Both values are much higher than reported from the auditory cortex of other mammals, with more than 51% of the units preferring modulation frequencies exceeding 100 Hz. Conspicuously, the fast modulations preferred by the neurons match the fast amplitude and frequency modulations of prosocial, and mostly of aggressive, communication calls in *P. discolor*. We suggest that the preference for fast amplitude modulations in the *P. discolor* dorsal auditory cortex serves to reliably encode the fast modulations seen in their communication calls.

NEW & NOTEWORTHY Neural processing of temporal sound features is crucial for the analysis of communication calls. In bats, these calls are often characterized by fast temporal envelope modulations. Because auditory cortex neurons typically encode only low modulation frequencies, it is unclear how species-specific vocalizations are cortically processed. We show that auditory cortex neurons in the bat *Phyllostomus discolor* encode fast temporal envelope modulations. This property improves response specificity to communication calls and thus might support species-specific communication.

amplitude modulation; auditory cortex; social communication; temporal processing

INTRODUCTION

The analysis of temporal sound features is one of the hallmarks of the auditory system of mammals and other vertebrates. Precise timing information about sound onset and envelope is essential for processing of interaural time differences for sound localization, but the analysis of temporal structure of sounds is also crucial for species-specific communication (Bohn et al. 2008). Temporal amplitude and frequency modulations are, among other sound features, important characteristics of human speech and animal communication sounds (Bohn et al. 2008; Gaucher et al. 2013; Nourski and Brugge 2011; Schwartz et al. 2007). Temporal processing in the auditory system has been intensively studied over the last decades for different stages of the ascending auditory pathway in different animal models (Joris et al. 2004; Langner 1992). Responses to sinusoidally amplitude-modulated (SAM) sounds can be quantified either in terms of a rate code or in terms of the synchronization of spikes to the modulator ("phase-locking"). It has been shown that the ability to encode temporal modulation in a phase-locked manner decreases from the auditory brain stem to the auditory cortex (AC). Neurons in the auditory nerve can follow the carrier up to around 10 kHz in owls (Köppl 1997) and up to 2 kHz in cats (Joris and Yin 1992). Yet, neurons in the inferior colliculus (IC) show phase-locking only up to 320 Hz in the rat (Rees and Møller 1987) and up to 500 Hz in Parnell's mustached bat (Burger and Pollak 1998). On the level of the AC, typically only modulation frequencies below 30 Hz in cats (Whitfield and Evans 1965) and guinea pigs (Creutzfeldt et al. 1980) and 35 Hz in macaques (Cohen et al. 2007) and marmosets (DiMattina and Wang 2006) are encoded with a phase-locked response. However, Hoglen et al. (2018) recently showed significant phase-locking in the AC of squirrel monkeys to modulation frequencies of up to 128 Hz. In comparison to the temporal modulation transfer functions (tMTF) responses in the AC, the rate modulation transfer functions (rMTF) responses usually extend to higher modulation frequencies. Yet, the majority of rate best modulation frequencies (rBMFs) in the AC of anesthetized animals are typically below 50 Hz (Eggermont 1998; Gaese and Ostwald 1995; Schreiner and Urbas 1988), although studies in awake animals have reported rBMFs exceeding this value (gerbils, Schulze and Langner 1997; squirrel monkeys, Bendor and Wang 2008; Bieser and Müller-Preuss 1996).

In bats, precise temporal processing is required to detect prey and avoid obstacles by echolocation. Numerous studies have revealed precise processing of echo delay and stimulus duration as the hallmark of the bat auditory system (Ehrlich et al. 1997; Greiter and Firzlaff 2017; Hagemann et al. 2010;

Address for reprint requests and other correspondence: S. G. Hörpel, Dept. of Animal Sciences, Technical University of Munich, Liesel-Beckmann-Str. 4, 85354 Freising, Germany (e-mail: stephen.hoerpel@tum.de).

Mittmann and Wenstrup 1995; Olsen and Suga 1991; O'Neill and Suga 1979; Sayegh et al. 2014). The neural structures in bats required for hearing are similar to those of other mammals and have simply been adapted to a more specialized role, i.e., echolocation (Covey 2005). Furthermore, neuronal responses to SAM and sinusoidally frequency-modulated stimuli in the bat auditory brain stem are not very different from those in other mammals (Covey et al. 1995; Grothe et al. 2001). This is astonishing, considering the rich vocal repertoire of these animals, which is often characterized by strong and fast temporal modulation or repetitive patterns of short sounds, especially in so-called distress and aggression calls (August 1979; Fenton et al. 1976; Gadziola et al. 2012; Hechavarría et al. 2016; Kanwal et al. 1994; Russ et al. 2004). In our animal model, the bat *Phyllostomus discolor*, the temporal amplitude modulation patterns of these calls are in the range of 100–130 Hz (Fig. 1*D*, *left* and *right*).

The representation of communication calls in the bat auditory system has been investigated in the AC (e.g., Esser et al. 1997; Washington and Kanwal 2008, 2012) and IC (Andoni et al. 2007; Andoni and Pollak 2011), as well as in the amygdala (Gadziola et al. 2012, 2016; Naumann and Kanwal 2011; Peterson and Wenstrup 2012). Neuronal responses were often influenced by the temporal modulation patterns and/or tempo-

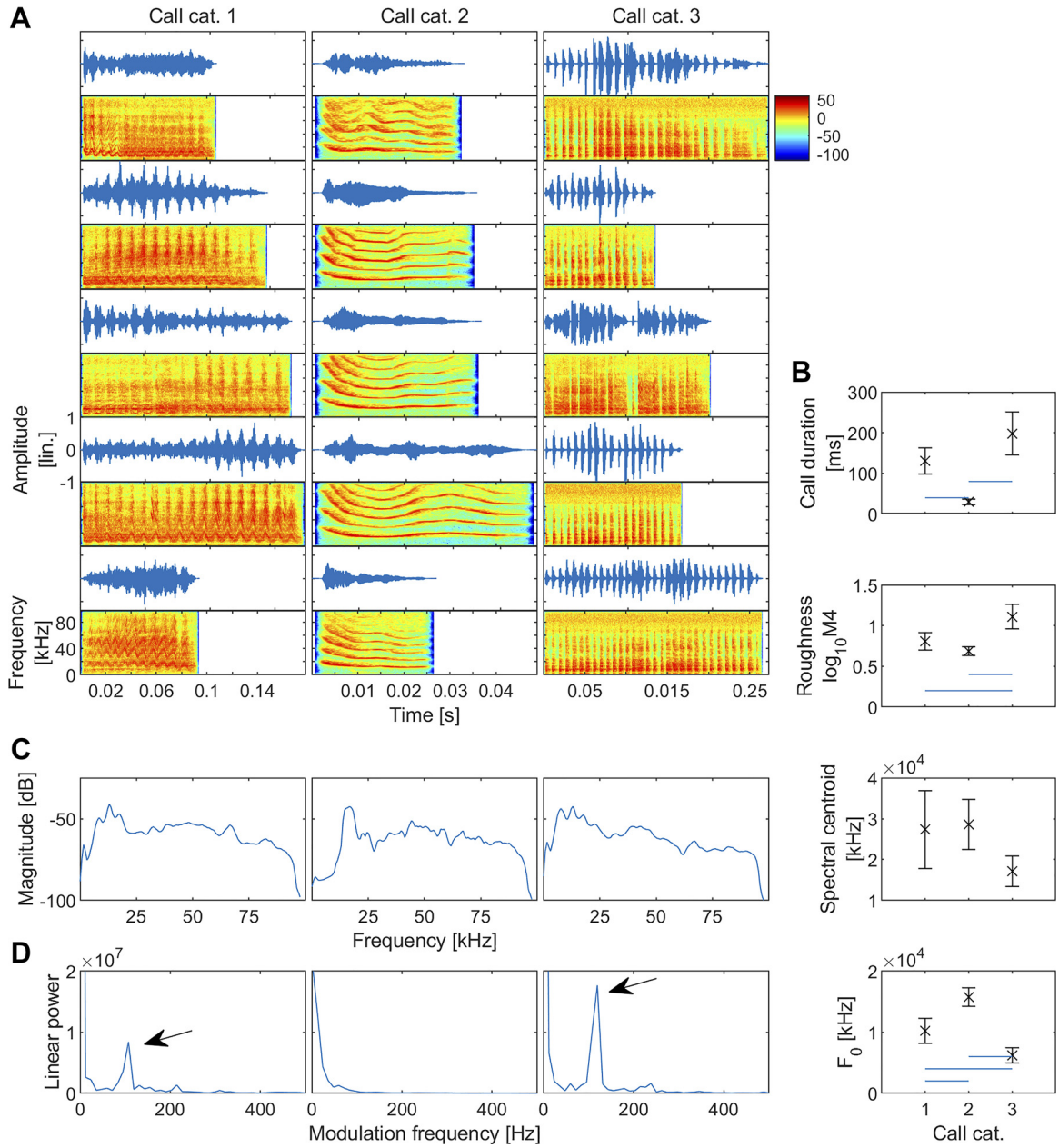

Fig. 1. Natural communication call categories of *Phyllostomus discolor* and their acoustic properties. *A*: waveforms and spectrograms of aggression calls (call *category 1* and call *category 3*) and appeasement/contact calls (call *category 2*) used as natural stimuli (cat., category). *B*: comparison of call duration, roughness ($\log_{10}$M4, where M4 = 4th moment of the envelope waveform), spectral centroid, and fundamental frequency (F_0) of the 3 call classes. Values are means (±SD). Blue lines indicate significant ($P < 0.05$, ANOVA) differences between call categories. *C*: frequency spectra of *category 1* (*left*), *category 2* (*middle*), and *category 3* (*right*) communication calls. *D*: amplitude modulation spectra of *category 1* (*left*), *category 2* (*middle*), and *category 3* (*right*) communication calls. Prominent peaks appear around 100–130 Hz in *category 1* and *category 3* (arrows) spectra. Note the lack of peak in call *category 2* spectrum.

ral order of syllable combinations. In the bat AC, communication calls were often encoded in areas that were also sensitive to a combination of echolocation calls and echoes separated by a certain delay and thus serving for target detection during echolocation (Esser et al. 1997; Kanwal and Ehret 2011; Kanwal and Rauschecker 2007). However, cortical neurons in bats could precisely encode the temporal envelope of SAM stimuli or naturalistic sequences of vocalizations up to frequencies around 20 Hz only (Jen et al. 1993; Martin et al. 2017). Recently, it was reported (García-Rosales et al. 2018a) that a subpopulation of units in the AC of *Carollia perspicillata* showed best synchronization to modulation frequencies of communication calls at roughly 60 Hz. Because temporal modulation patterns of behaviorally relevant communication calls were reflected in the response patterns of neurons in the primary AC of other mammals (Nagarajan et al. 2002; Wang et al. 1995), this raises the question how the fast temporal modulation found in bat communication sounds are represented in the AC.

We investigated the coding of temporal envelope modulation in neurons of the non-tonotopic dorsal fields of the AC of the bat *P. discolor*. By measuring rMTFs and tMTFs in response to SAM stimuli, we could show that a population of cortical neurons had an rBMF of around 130 Hz, whereas the temporal best modulation frequency (tBMF) peaked at 87 Hz, and had 50% cutoff frequencies up to 230 Hz. This ability to encode surprisingly fast temporal modulations might be an adaptation to the fast modulations found in certain types of species-specific communication calls and, so far, has not been reported for other bat species.

METHODS

Surgery

All the experiments complied with the principles of laboratory animal care and were conducted following the regulations of the current version of the German Law on Animal Protection (approval ROB-55.2-2532.Vet_02-13-147, Regierung von Oberbayern). The bats (*P. discolor*; 3 adult females, 1 adult male) originated from a breeding colony situated in the Department of Biology II of the Ludwig-Maximilian University of Munich. For experiments, animals were kept separated from other bats under seminatural conditions (12:12-h day-night cycle, 65–70% relative humidity, 28°C) with free access to food and water.

The surgical procedures are described in detail in a previous publication (Hoffmann et al. 2008) and will be mentioned only briefly. The bats were anesthetized using a combination of medetomidine (Dorbene; Zoetis), midazolam (Dormicum; Hoffmann-La Roche), and fentanyl (Fentadon; Albrecht) at dosages of 0.4, 4.0, and 0.04 μg/g body wt, respectively. Anesthesia was maintained through additional injections containing two-thirds of the initial dose every 1.5 h. The skin overlying the skull was opened along the midline, and the skull surface was freed from tissue. A small metal tube was then fixed to the skull using a microglass composite to fix the animal to a stereotaxic device. Details of the stereotaxic device and the procedure used to reconstruct the recording sites are described elsewhere (Schuller et al. 1986). In brief, the alignment of the animal's skull and the underlying brain within the stereotaxic coordinate system was measured by scanning the characteristic profile lines of the skull in the parasagittal and frontal planes. These profiles were then digitally fitted to a standardized skull profile in a standardized coordinate system.

To alleviate postoperative pain, an analgesic (0.2 μg/g body wt meloxicam; Metacam; Boehringer-Ingelheim) was administered after the surgery for 4 postoperative days. The anesthesia was antagonized with a mixture of atipamezole (Alzane; Novartis), flumazenil (Flumazenil; Hexal), and naloxone (Naloxon-ratiopharm; Ratiopharm), which was injected subcutaneously (2.5, 0.5, and 1.2 μg/g body wt, respectively). The bats were treated with antibiotics (0.5 μg/g body wt enrofloxacin; Baytril; Bayer) for 4 postoperative days.

Acoustic Stimulation

To measure the neuronal response properties to SAM sounds, the following procedure was used: a frequency-response curve of the neuron under test was established by presenting pure tone stimuli with a frequency range from 5 to 80 kHz (logarithmically spaced in ⅛ octave steps) and with sound pressure level (SPL) from 80 to 15 dB referenced to 20 μPa. The duration of each pure tone was 20 ms, and the stimuli were preceded by 50 ms of silence. The repetition rate was 2 Hz. The neuronal response was measured in a response window starting at stimulus onset and lasting 250 ms. The stimuli were each presented in random order and repeated 10 times. The data were plotted using the BrainWare analysis tools [Tucker-Davis Technologies (TDT), Gainesville, FL], and the characteristic frequency (CF; frequency at which a given neuron responds to the lowest sound intensity) and corresponding threshold SPL were identified. To create the SAM stimuli, a 400-ms (t) pure tone carrier (f_c) at the CF of the unit was modulated with 15 different modulation sinusoids (f_m) logarithmically spaced from 5 to 1,500 Hz, as shown in Fig. 2. The modulation depth (m) was 100% (*Eq. 1*; Joris et al. 2004).

$$\left[1 + m\sin\left(2\pi f_m t\right)\right]\sin\left(2\pi f_c t\right) \quad (1)$$

The modulation frequencies were each randomly presented 20 times at 10–15 dB above the CF SPL. Each stimulus was preceded by a 50-ms silent period. Repetition rate was ~1.1 Hz.

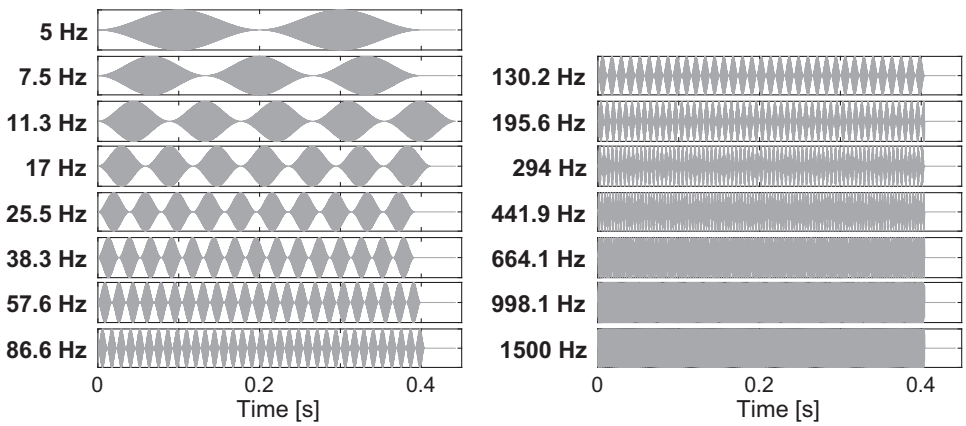

Fig. 2. Sinusoidally amplitude-modulated (SAM) stimuli. Waveforms of the SAM stimuli are shown (carrier frequency, 20 kHz) at modulation frequencies of 5–1,500 Hz in 15 logarithmically spaced steps (modulation depth 100%). Note small variations in stimulus length to permit full modulation cycle.

Communication Calls

To test whether neuronal responses to SAM sounds could be related to responses of communication sounds, we presented 15 *P. discolor* communication sounds (Fig. 1*A*). The sounds were selected from a library of 269 calls recorded in the *P. discolor* colony in the Department of Biology II of the Ludwig-Maximilian University of Munich.

The 15 selected communication sounds were grouped into three categories on the basis of differences in several acoustic parameters such as duration, fundamental frequency F_0, roughness (Fig. 1*B*), and occurrence of amplitude and frequency modulations in the call envelope and spectrogram, respectively (Fig. 1*D*). *Category 1* calls consisted of long amplitude and frequency-modulated calls with relatively low fundamental frequency of ~13 kHz (see Fig. 1*C*, *left*), whereas the amplitude modulation spectrum showed a peak around 100–130 Hz (Fig. 1*D*, *left*). *Category 2* calls showed no amplitude modulations, were shorter in duration, had a higher fundamental frequency of ~17 kHz and a strongly harmonic spectrum, and displayed shallow frequency modulations (Fig. 1*D*, *middle*). *Category 3* calls consisted of a varying number of short broadband sound elements separated by ~8 ms and thus giving rise to strong amplitude modulations. In contrast to *category 1* calls, *category 3* calls showed no frequency modulations and had a significantly lower fundamental frequency of ~7.5 kHz. Similarly to *category 1* calls, *category 3* calls also displayed a peak amplitude modulation frequency of 100–130 Hz (Fig. 1*D*, *right*). Unlike the fundamental frequencies of the respective call categories, the spectral centroid did not differ significantly between the categories. The roughness values ($\log_{10}$M4; Fig. 1*B*) are given as the base 10 logarithm of the envelope roughness, which was quantified in terms of the fourth moment (M4; the envelope waveform raised to the power of 4 divided by the squared waveform raised to the power of 2; Firzlaff et al. 2006; Hartmann and Pumplin 1988). The envelope roughness of *category 3* calls is significantly higher than that of the other two call categories. The calls were randomly presented with 20 repetitions (repetition rate ~0.7 Hz) at a level of ~15–20 dB above CF threshold.

Because a comprehensive call repertoire of social calls has not been published for *P. discolor*, clear assertions about the behavioral context of the calls recorded in the present study are not possible. However, calls of *category 1* and *category 3* resembled typical aggression and distress calls as described for other bat species (Gadziola et al. 2012; Hechavarría et al. 2016). *Category 2* calls resembled maternal contact calls or appeasement calls of *P. discolor* (Esser and Schubert 1998) and other bat species (Gadziola et al. 2012).

Electrophysiological Recordings

After initial surgery, experiments were conducted in a sound-attenuated and heated (~35°C) chamber. Extracellular recordings were made with parylene-coated tungsten microelectrodes (5-MΩ impedance; Alpha Omega) in anesthetized bats (see *Surgery*). Note that the responses recorded from cortical units under this anesthesia regime reflect the behavioral performance of *P. discolor* well (Firzlaff et al. 2006). Recording sessions took place 3 days per week for up to 8 weeks (with at least 1 day off between consecutive experiments) and could last up to 5 h per day. Dorsoventral (DV) electrode penetrations in the AC were run obliquely to the brain surface with different mediolateral (ML) and rostrocaudal (RC) angles. The electrode signal was recorded using an analog-to-digital converter (TDT RA16 and RX5; sampling rate 25 kHz, bandpass filter 400-3,000 Hz) and BrainWare (TDT). The action potentials were threshold discriminated and saved for later offline analysis. We tried to isolate single neurons whenever possible; however, it was not always possible to clearly discriminate the activity of a single neuron. Therefore, the term "unit" is used in this article to describe the collective activity of one to three neurons recorded at a recoding site. A comparison of neuronal responses from single units and multiple units revealed no differences.

To search for acoustically driven neural activity, either a natural echolocation call (downward modulated, multiharmonic, main energy between 40 and 90 kHz, duration ~1.2 ms) or an aggression call (frequency and amplitude modulated, main energy between 0 and 20 kHz, duration ~170 ms) was presented periodically. During the search, the SPLs were varied while neural activity was monitored visually and acoustically. All acoustic stimuli were computer generated (MATLAB; The MathWorks, Natick, MA), digital-to-analog converted (TDT RX6; sampling rate 195,312 Hz), attenuated (TDT PA5), amplified (Yamaha AX-396), and presented via a free-field loudspeaker (Scan-Speak R2904-7000-00), which had been calibrated for linear frequency response between 1 and 95 kHz. The loudspeaker was positioned contralaterally ~30° off the head midline at a distance of ~20 cm, and the search stimuli were presented with a repetition rate of 2 Hz. After the experiments were completed, a neuronal marker (BDA 3000; Sigma-Aldrich; 1 mg/20 μl phosphate buffer) was pressure-injected (Nanoliter 2010 injector; World Precision Instruments) into the brains to reconstruct the position of the recording sites in standardized stereotaxic coordinates (Schuller et al. 1986) of a brain atlas of *P. discolor* (Nixdorf A, Fenzl T, Schwellnus B, unpublished observations). The animals were then euthanized by an intraperitoneally applied lethal dose of pentobarbital sodium (0.16 mg/g body wt) and subsequently perfused transcardially with 4% paraformaldehyde.

Data Analysis

Spike responses from the 15 SAM and 15 natural stimuli were displayed as peristimulus time histograms (PSTHs; bin width 1 ms) and raster plots. Few units showed spontaneous activity and, when present, the spontaneous spike rate was very low (<10 spikes/s). For the natural stimuli, the mean spike rates of the neuronal responses to aggression (call *categories 1* and *3*, R_{agg}) and appeasement/contact calls (call *category 2*, R_{cont}) were calculated over a 400-ms response window, starting at the stimulus presentation. By using *Eq. 2* (Schnupp et al. 2006; Wang et al. 1995; Wang and Kadia 2001), the "selectivity index" d_i of each unit was calculated.

$$d_i = \frac{R_{agg} - R_{cont}}{R_{agg} + R_{cont}} \quad (2)$$

The d_i ranges from +1 to −1, indicating a neuron responding only to the aggression call (+1) or only to the contact call (−1), with a 50% difference between R_{agg} and R_{cont}, resulting in a d_i value of ±0.3.

In the case of SAM stimuli, rMTFs were constructed by plotting the median response rate (for 20 repetitions) calculated in a fixed PSTH window (from 50 to 450 ms, 1-ms binning) over modulation frequency. Because many units responded to the onset of a SAM stimulus with a strong phasic response, onset responses were eliminated for the construction of temporal modulation transfer functions (tMTFs) as suggested by Heil et al. (1995). To do so, the response window was adjusted to remove the response to the first modulation cycle for each modulation frequency. The ability of the units to synchronize spikes to the modulation frequency of SAM stimuli was measured using the vector-strength (VS) analysis in *Eq. 3* (Goldberg and Brown 1969; Martin et al. 2017).

$$VS = \frac{\sqrt{(\sum x_i)^2 + (\sum y_i)^2}}{n} \quad (3)$$

The VS values ranged from 0 (homogenous spike distribution across stimulus period) to 1 (perfect synchronization, all spikes occurring at same stimulus phase). Rayleigh's test (Buunen and Rhode 1978) with $P \leq 0.01$ was used to test the significance of the vector strength. Nonsignificant responses were set to 0. To finally yield the tMTF, the VS was plotted over modulation frequency. In rare cases ($n = 3$; ~2%), phase-locking occurred to every second modulation cycle for higher modulation frequencies. These units were omitted from tMTF

calculations. rMTFs were classified as bandpass, high pass, low pass, or unspecific. Bandpass rMTFs were characterized by a decrease of the spike rate of at least 50% on both sides of the maximum. High-pass and low-pass rMTFs had a decrease of spike rate of at least 50% on only one side (the low or the high modulation frequency side, respectively), but not on the other side. Unspecific rMTFs lacked a 50% decrease on either side of the maximum. To quantify the 50% cutoff values of rMTFs, polynomials were fitted to the flanks of the functions and the 50% point between the highest and lowest rate was determined on each polynomial. tMTFs were classified accordingly.

To see if the envelope modulation of *P. discolor* communication calls is reflected in the temporal spike pattern of cortical units, the temporal response properties to aggression and appeasement/contact calls of *P. discolor* were analyzed by computing the PSTH autocorrelation (PSTH 1-ms binning) and subsequently extracting spectral information (Wang et al. 1995). The call envelopes were extracted via Hilbert transformation and were smoothed with a second-degree Butterworth filter. Following this step, we compared frequency components of both the call envelope spectrum and the PSTH autocorrelation spectrum around 100–130 Hz using a multitaper method [MATLAB *pmtm* function; confidence level 0.95, time-halfbandwidth product (*nw*) 4, sample rate 192 kHz, fast Fourier transform size determined by length of the signal]. If repetitive firing of the units occurred following the temporal envelope of the aggression calls, a significant peak could be detected in this frequency range.

RESULTS

In total, we recorded from 142 units from both hemispheres of the AC of *P. discolor* [4 adult animals: 3 females (102 units) and 1 male (40 units)]. Recordings were derived mainly from cortical layers III and IV. As shown in Fig. 3, the majority of the units recorded were located in the anterior dorsal (ADF) and posterior dorsal fields (PDF; Hoffmann et al. 2008). The CFs of the recorded units overlapped with the fundamental frequencies of the vocalizations with a median CF of 20 kHz (mean 32.9 kHz) and with the maximum of the CF distribution at 18 kHz. As expected from previous studies (Hoffmann et al. 2008), there was no correlation between the RC position and the CF of the units in the dorsal AC.

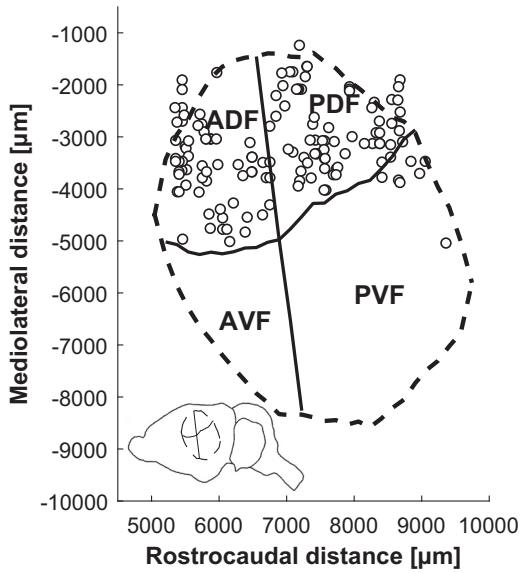

Fig. 3. Recording sites and subfields in the auditory cortex (AC) of *Phyllostomus discolor*. Shown are projections of recording sites (circles) on an unrolled and flattened cortical surface with schematic AC subfields: anterior dorsal field (ADF), posterior dorsal field (PDF), anterior ventral field (AVF), and posterior ventral field (PVF). *Inset* shows overall position of the AC in the brain of *P. discolor*.

Neuronal Response Classes to SAM Stimuli in the Dorsal AC

Neuronal responses to SAM stimuli were assigned to six different classes, based on the type of the rMTF (bandpass, high pass, low pass, all pass) and the temporal response pattern (on response, tonic response, phase-locked response).

Class I units ($n = 38$; Fig. 4) had a bandpass rMTF. The temporal response pattern was characterized by a phasic on response followed by a prolonged response component that showed significant phase-locking to a limited range of modulation frequencies.

Class II units ($n = 33$; Fig. 4) also had a bandpass rMTF, but the temporal response pattern lacked the onset response and phase-locking behavior. Instead, responses consisted of a tonic component.

Class III units ($n = 22$; Fig. 4) were not selective for certain modulation frequencies but responded equally to all SAM stimuli (all pass). Temporal response patterns were tonic without onset response and phase-locking.

Class IV units displayed high-pass rMTFs ($n = 25$; Fig. 4). These units showed either pure onset responses, an additional tonic response component or displayed a tonic response pattern only.

A tonic response pattern and a low-pass rMTF were found in *class V* units ($n = 4$; Fig. 4). Units in *classes IV* and *V* did not show phase-locking to SAM stimuli.

Finally, a number of units ($n = 20$; not shown) displayed rMTFs and/or temporal response patterns that were not unequivocally classifiable by our criteria. These units were labeled *class VI* and excluded from any further calculations.

The population of bandpass units (*class I* and *class II*) recorded had a median best rate response at 86.6 Hz [interquartile range (IQR) = 91.8 Hz] with a peak at 130-Hz modulation frequency (Fig. 5*A*). The median 50% lower cutoff frequency was 23 Hz, and the median 50% upper cutoff frequency was 241 Hz for the rate response. In detail, *class I* bandpass units had a median best rate response of 86.6 Hz (IQR = 91.8 Hz), whereas *class II* bandpass units reached a median best rate response of 130.2 Hz (IQR = 93.7 Hz).

The calculation of a median rate response in units with an onset response and/or high-pass rMTFs is futile, because it would highly depend on the range of modulation frequency tested. Therefore, we only show the lower 50% cutoff value for *class IV*: 24 Hz (IQR = 33.3 Hz). The low-pass *Class V* units had a median best rate response of 7.5 Hz (IQR = 40.8 Hz).

Furthermore, of the 122 units included in the calculations, 35 units (i.e., *class I*, 28.7%) showed significant phase-locking according to the VS analysis. The median highest frequency that evoked phase-locking was 130.2 Hz (Fig. 5*B*; IQR = 65.5 Hz), with the median best phase-locking frequency being 25.5 Hz (IQR = 44.9 Hz). The median 50% upper cutoff frequency for phase-locking was 162.9 Hz (IQR = 81.9 Hz).

Neuronal Responses to Communication Calls

Call selectivity. The selectivity index d_i quantifies the selectivity of a unit for either aggressive calls (*category 1* and

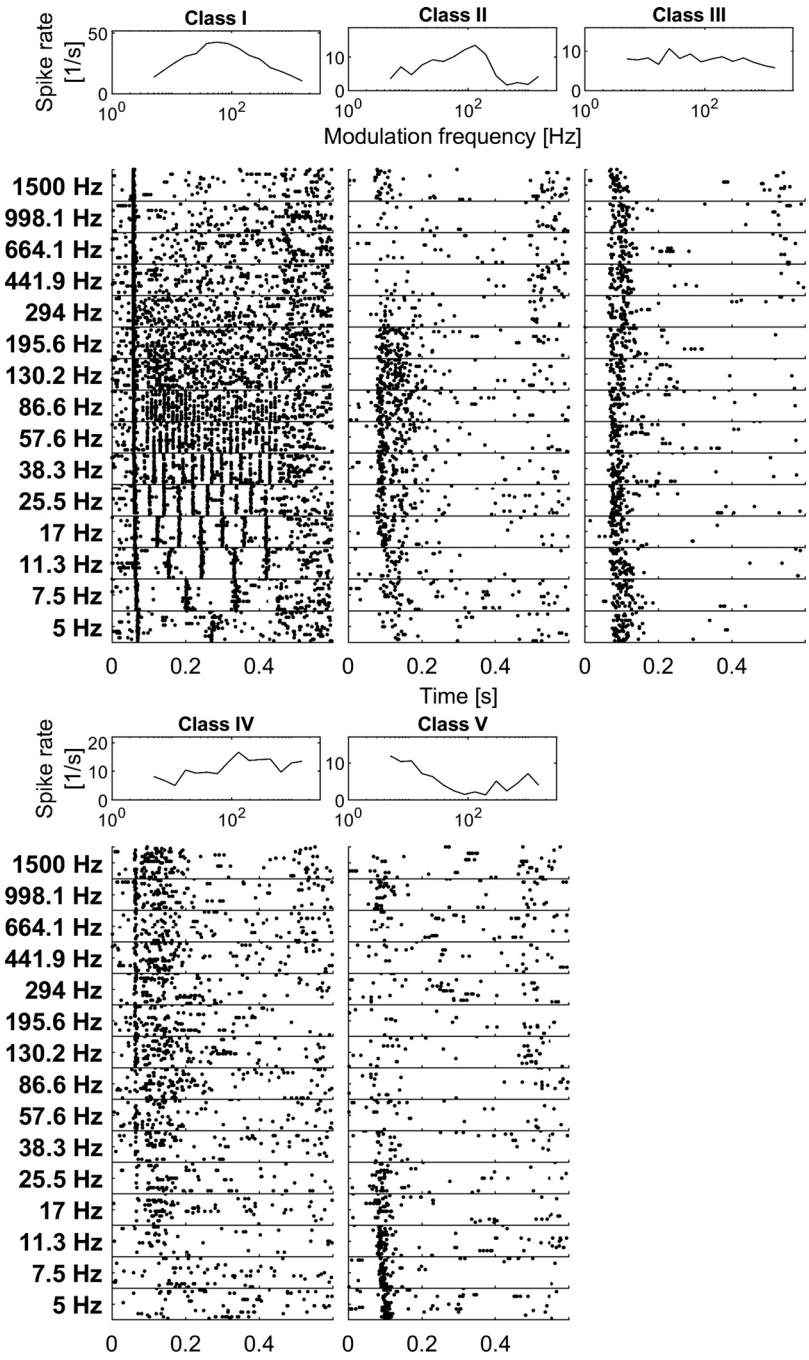

Fig. 4. Response classes of cortical units. Representative examples are rate modulation transfer functions (rMTFs) and raster plots of the 5 different response classes. *Class I* and *class II* units have bandpass rMTFs with phasic onset responses and significant phase-locking to a limited range of modulation frequencies (*class I*) or tonic responses lacking the onset response and phase-locking behavior (*class II*). *Class III* units have tonic, nonselective, all-responsive units lacking onsets and phase-locking. *Class IV* units have high-pass rMTFs. *Class V* units have low-pass rMTFs.

category 3) or contact calls (*category 2*). A total of 61 units (50%) had a strong preference for the aggression calls ($d_i \geq 0.3$). Only 4 units (3.3%) had a negative d_i value and thus showed preference toward the contact/appeasement calls, whereas 57 units (46.7%) showed no selectivity or only a small preference toward the aggression calls ($0 \leq d_i < 0.3$). The mean d_i value of all recorded units was 0.3153 ± 0.2055 (median $d_i = 0.3011$).

Call selectivity of different SAM response classes. To see if the units' call-type preferences are related to the response classes for SAM stimuli, we plotted their selectivity indexes against their corresponding response classes, which is depicted in a heat map (Fig. 6). For simplification, the negative d_i values were grouped with all the other values <0.1 and their respective d_i values were set to 0. Of the 61 units with a selectivity index exceeding the median d_i value of 0.3011, 35 units ($>57\%$) responded in a bandpass manner, and the phase-locked bandpass units in particular exhibited higher than average selectivity. In other words, if units showed a high degree of call selectivity, they most probably had bandpass rMTFs.

Furthermore, we checked for an existing correlation between the best rMTF frequency and the selectivity index d_i. In Fig. 7*A*, the best rMTF frequencies of *class I* (*left*) and *class II* (*right*) band pass units were plotted against their respective d_i values. It can be seen that *class I* units with higher best rMTF frequencies also show increased selectivity toward aggression calls (Pearson correlation coefficient $r = 0.69$, $P < 0.00001$). *Class II* units also show an increased selectivity toward these

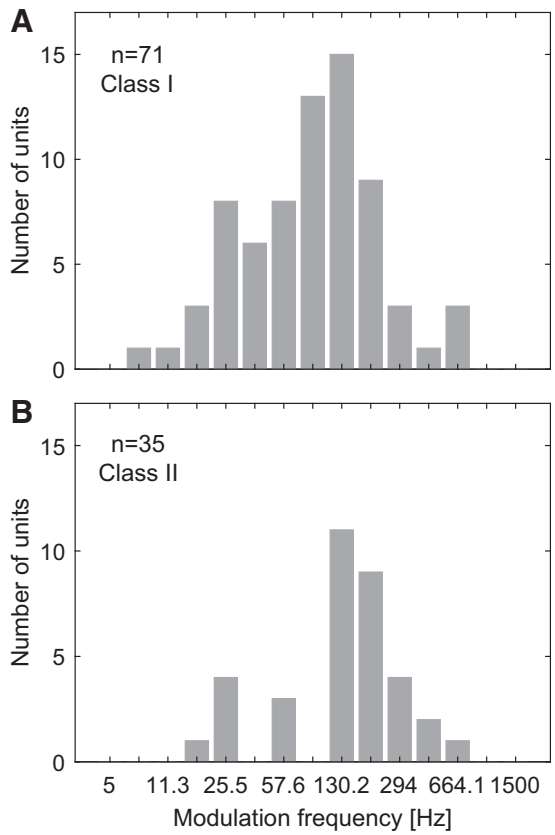

Fig. 5. Distribution of best rate modulation transfer function (rMTF) and highest temporal modulation transfer function (tMTF) bandpass units. *A*: histogram of the best modulation frequencies (BMF) of the rMTF of the 71 *class I* and *class II* bandpass units. The median best rate response is at 86.6 Hz with a maximum of the distribution at 130-Hz modulation frequency. *B*: histogram of the highest phase-locking frequency of the 35 *class I* bandpass units (3 units were omitted because they phase-locked to every 2nd modulation cycle for higher modulation frequencies). The median highest phase-locked response and the maximum of the distribution are at 130-Hz modulation frequency.

calls; however, in this case, the correlation between the best rMTF frequencies of the units and their selectivity is weaker ($r = 0.41$, $P = 0.0166$).

Cortical distribution of bandpass rMTFs. Additionally, we also investigated the relationship between the different neuronal classes and their corresponding position in the AC of *P. discolor*. In Fig. 7*B*, the RC and DV distances of *class I* (*left*), *class II* (*right*), and *class III–V* units (*left and right*) can be seen. In both plots of Fig. 7*B*, there is a conspicuous accumulation of bandpass-type units in the more caudal and dorsal parts of the AC, which is highly significant (2-sample *t*-test, $P < 0.001$; Fig. 7*C*). This dorsocaudal region corresponds roughly to the PDF of the AC of *P. discolor* (Hoffmann et al. 2008; see also Fig. 3 for outlines of cortical fields).

Call selectivity and temporal spike pattern. Finally, we analyzed if envelope modulation of *P. discolor* communication calls is reflected in the temporal spike pattern of cortical units. In Fig. 8*A*, one can see the waveform of a typical aggression call (call *category 3*) and its corresponding envelope (Fig. 8*B*). The response of a cortical unit to this specific call is depicted in Fig. 8*C*, and one can see that the neural responses phase-lock to the envelope of the communication call. By comparing the spectrum of the autocorrelation of the units' response PSTH (Fig. 8*D*) with the envelope modulation spectra (Fig. 8*E*), this becomes even clearer, because both spectra show distinct peaks between 100 and 130 Hz. In other words, several units locked to the envelope precisely and thereby encoded its modulation frequency. A total of 18 units (14.8%) showed peaks in the PSTH autocorrelation spectra as a response either to *category 1* or *3* calls or to calls from both categories. In detail, four units (3.3%) showed peaks in the PSTH autocorrelation spectra as a response to *category 1* calls and one unit (0.8%) as a response to *category 2* calls, whereas all units (18 units, 14.8%) showed peaks in the PSTH autocorrelation spectra as a response to *category 3* calls. Only a single unit showed responses to all three call categories. The median selectivity index d_i values of units preferring *category 1* or *category 3* calls are noticeably higher than the median d_i value of all units [0.3794 (*category 1*) or 0.3763 (*category 2*) vs. 0.3011]. Furthermore, 16 of the 18 units belonged to the group of *class I* bandpass units. In summary, units that phase-locked to the call envelope could better differentiate between aggressive and nonaggressive communication calls.

DISCUSSION

The present study investigated coding of temporal sound features in cortical units of the bat *P. discolor*. Responses to SAM sounds revealed the ability of a population of units to encode high modulation frequencies (100–130 Hz) in their firing rate but also as temporal code in phase-locked spike patterns. These units often preferably responded to communications calls used in an aggressive context, which are characterized by temporal envelope modulations around 130 Hz. In the following we compare our findings in *P. discolor* with results on temporal processing in other bats and other mammals, discuss possible neuronal mechanisms in *P. discolor* that might lead to the observed ability to encode fast temporal modulations of sound envelope, and depict possible functional

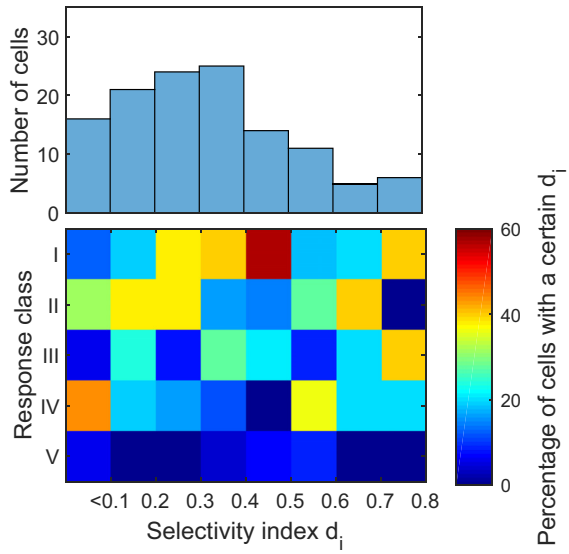

Fig. 6. Call class selectivity of sinusoidally amplitude-modulated (SAM) stimuli response classes. Heat map (*bottom*) shows the units' selectivity index d_i plotted against the 5 response classes with histogram (*top*) shown to visualize the distribution of the units (mean d_i of the units = 0.3153). The color bar indicates the percentage of units within a certain d_i range; the majority of the units are *class I*, *II*, and *III* types.

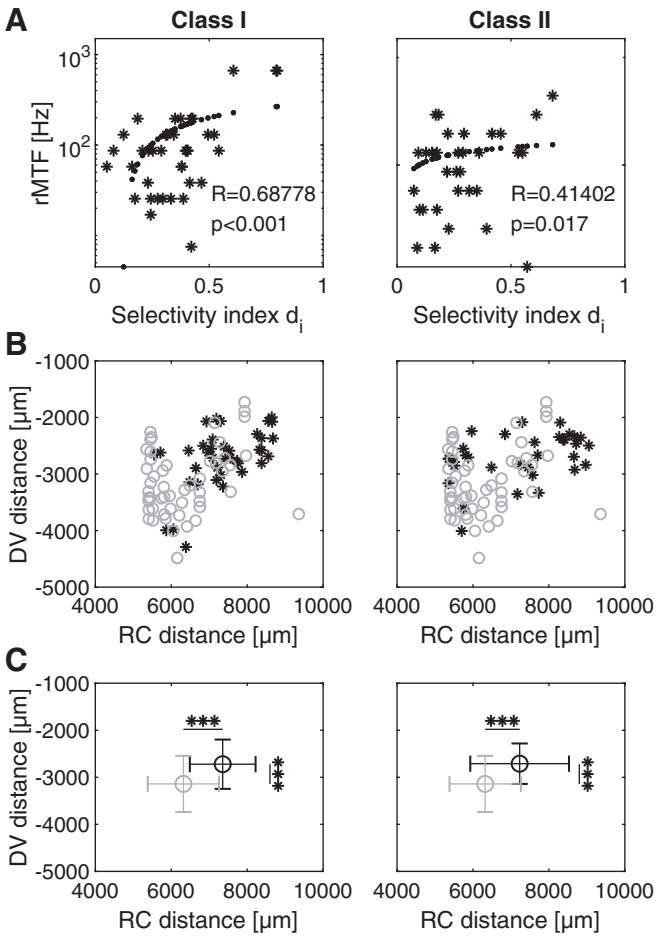

Fig. 7. Correlation of selectivity index and best rate modulation transfer function (rMTF) of *class I* and *class II* bandpass units and their spatial position in the auditory cortex (AC). *A*: correlation of selectivity index d_i plotted against the best rMTF of *class I* (*left*) and *class II* (*right*) bandpass units with regression curve indicated as a dotted line. *B*: rostrocaudal (RC) distance plotted against dorsoventral (DV) distance for *class I* (*left*; asterisks) and *class II* (*right*; black asterisks) compared with *class III–V* units (*left* and *right*; gray circles). *C*: mean RC distance plotted against mean DV distance with added standard deviations for *class I* (*left*, black error bars) and *class II* (*right*; black error bars) compared with *class III–V* units (*left* and *right*; gray error bars). The accumulation of the *class I* and *class II* units in the more caudal parts of the AC (mainly the posterior dorsal field) is highly significant (***$P < 0.001$, 2-way *t*-test).

implications of our findings for neural processing of vocal communication.

Temporal Processing in the AC of Bats and 0

In most studies, the range of rBMFs in the AC of mammals is limited to modulation frequencies below 50 Hz (Joris et al. 2004; Martin et al. 2017; Schreiner and Urbas 1988), although exceptions are possible (Schulze and Langner 1997). Phase-locked responses are typically also observed up to this range (Creutzfeldt et al. 1980; Whitfield and Evans 1965). So far, results from the AC of bats did not differ from findings from other mammals: in most (~89%) cortical units of *C. perspicillata*, a species closely related to *P. discolor*, significant phase-locking to the sound envelope was observed only below 23 Hz (García-Rosales et al. 2018b), although it was recently reported for the same species that 25% of units in the AC showed best synchronization to modulation frequencies of communication calls at roughly 60 Hz (García-Rosales et al. 2018a). In *Myotis lucifugus*, most units could not exceed phase-locking frequencies of 30 Hz (Condon et al. 1997). In the big brown bat *Eptesicus fuscus*, units in the AC could only follow pulse trains up to 10-Hz repetition frequency (Jen et al. 1993). These findings are somewhat surprising because for the bat bio-sonar systems, high temporal resolution is crucial to the precise detection of obstacles and prey. Indeed, units in the so-called chronotopic map of bats are sharply tuned to best delays between emitted echolocation calls and reflected echoes as short as 1 ms (Bartenstein et al. 2014; Hechavarría et al. 2013; O'Neill and Suga 1979).

Martin et al. (2017) investigated SAM coding in the primary AC of *C. perspicillata*. In contrast, our present study in *P. discolor* investigated units in the nonprimary dorsal fields (Hoffmann et al. 2008) of the AC. The chronotopic delay map in *P. discolor* is located in the PDF (Greiter and Firzlaff 2017), and most units with bandpass rMTFs with peaks around 130 Hz and high phase-locking abilities were located in this field, too (see Fig. 3 and Fig. 7, *B* and *C*). The vocal communication repertoires of *C. perspicillata* and *P. discolor* are quite similar (Hechavarría et al. 2016; compare Fig. 1), and both bats are

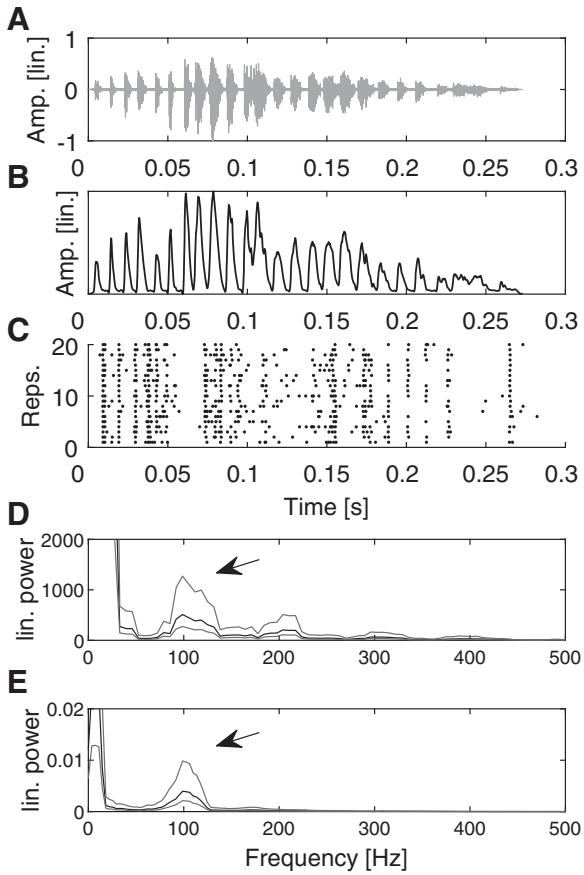

Fig. 8. Encoding of natural call envelope modulation frequency. *A*: temporal waveform of a *P Phyllostomus discolor* aggression call (spectrum from Fig. 1*A*, call *category 3*, 1st call). *B*: temporal envelope of the aggression call shown in *A*. *C*: raster plot of the corresponding neuronal response to the call shown in *A*. *D*: modulation spectrum of the peristimulus time histogram autocorrelation of the neuronal response shown in *C*. Gray lines are 0.95 confidence level borders. *E*: modulation spectrum of the call envelope shown in *B*. Gray lines are 0.95 confidence level borders. Both spectra (*D* and *E*) show distinct peaks between 100 and 130 Hz (arrows).

phylogenetically closely related and share many of their ecological preferences. Therefore, the profound differences in the responses to SAM sounds might be attributed to differences in the neural circuitry of the primary and nonprimary dorsal fields. However, one must be aware that coding of SAM sounds and coding of call-echo delay are thought to be based on different neuronal mechanisms.

Neuronal Mechanisms of Temporal Envelope Coding

As shown in RESULTS, we found two types of units with a bandpass response pattern caused by different mechanisms. Generally, a neuron with a phase-locked response will not respond to modulation frequencies exceeding its upper cutoff limit, thereby creating a typical bandpass modulation transfer function (see Fig. 4, *class I*). Additionally, units with pure rate responses can also show this characteristic, decreasing their spike rate/count after leaving their preferred frequency range (see Fig. 4, *class II*).

Rate responses of units in the cochlear nucleus are typically not tuned to certain modulation frequencies, but modulation frequency is encoded as a temporal code (Rhode and Greenberg 1994). On later stages of the ascending auditory pathway, rMTFs become generally more diverse and are created by multiple neuronal interactions (e.g., Heil et al. 1995; Krishna and Semple 2000). Synchronized excitatory inputs have been discussed as a mechanism for this at the level of the IC (Hewitt and Meddis 1994; Krishna and Semple 2000), although inhibition might contribute to the shape of rMTFs by suppressing responses to certain modulation frequencies. A model for low-pass responses proposed for the medial superior olive in mustached bats by Grothe (1994) is based on inhibitory inputs delayed with respect to excitation by a constant amount. Depending on modulation period, inhibitory and excitatory inputs might temporally overlap and thus restrict the range of modulation frequencies to which the neuron is responsive.

For the stages of the auditory pathway above the IC, Eggermont (1996) suggested that the tBMF is mainly determined by processes intrinsic to the cortical-thalamic network, whereas intrinsic pyramidal cell mechanisms influence the cutoff frequency. Furthermore, Eggermont (2002) described two main components of the envelope synchronization, i.e., the degree of input/presynaptic synchrony and shape of the temporal filter, which in turn is determined by properties of synaptic dynamics.

In contrast to SAM stimuli coding, delay tuning in bats is first observed on the level of the IC (Mittmann and Wenstrup 1995) and is created by spectrotemporal integration of inputs from the lateral lemniscus. Neural mechanisms for creating delay sensitivity employ coincidence of glycinergic postinhibitory rebound facilitation (Sanchez et al. 2008), but paradoxical latency shifts are also discussed as mechanisms for delay tuning in other bats (Feng 2011; Hechavarría and Kössl 2014; Sullivan 1982). Interestingly, Hechavarría and Kössl (2014) suggested that cortical units in the bat *C. perspicillata* might inherit delay-tuning properties from auditory stations below the AC. Following this line of argumentation, a possible (although hypothetical) explanation for the unusually high best modulations frequencies in rMTFs and tMTFs observed in our study can be supposed: temporal modulation properties of IC units might mainly be passed without further modification to the dorsal AC in *P. discolor*. This might therefore represent a fundamental scheme for this area. This hypothesis is supported by the fact that the dorsal field of AC in other bats often receive input from different subregions of the auditory thalamus (i.e., the medial geniculate body) than the primary cortex (Radtke-Schuller et al. 2004). Special functional properties in terms of temporal processing might come with those special thalamocortical connections. This was also recently suggested for the fast synchronization of local field potentials of cortical units in the AC of *C. perspicillata* (García-Rosales et al. 2018a). Furthermore, it might also be possible that coding of fast amplitude modulation in the PDF of *P. discolor* is facilitated by the temporal delay-tuning properties often found in neurons of this cortical region. Delay tuning of neurons in the chronotopic map of *P. discolor* is well observed in the range around 10 ms (Greiter and Firzlaff 2017). These neurons might therefore be preadapted to the processing of temporal envelope modulations in the frequency range around 100 Hz. Fast envelope modulation coding observed in our study might thus be considered to be an epiphenomenon, explaining the different results of our study and the study of Martin et al. (2017) in the primary AC of *C. perspicillata*.

Possible Influence of Anesthesia

In this study, we used a combination of medetomidine, midazolam, and fentanyl. Medetomidine did not produce an observable effect on neural activity in the IC and the primary AC of the Mongolian gerbil (Ter-Mikaelian et al. 2007). Immunoreactivity for endogenous opioids such as enkephalin is generally low or absent in the primary AC and the medial geniculate body but is abundant in other nuclei of the auditory pathway (Aguilar et al. 2004; Robertson and Mulders 2000). The main effect of enkephalin seems to be inhibition of the cochlear neural output via the descending olivocochlear bundle (Bürki et al. 1993). Thus the opioid fentanyl used in our study might have had a nonspecific overall inhibitory effect on neural activity to acoustic stimulation.

Midazolam, like other benzodiazepines, enhances $GABA_A$-mediated inhibition and might be the main source of possible anesthesia effects in this study. Temporal processing was influenced by GABAergic disinhibition in that the phase-locking ability of bat IC neurons was increased (Lu et al. 1998). In addition, anesthesia with pentobarbital sodium (which also enhances $GABA_A$-mediated inhibition) reduced stimulus-induced activity in neurons in the rat AC (Gaese and Ostwald 2001). The use of midazolam in our study might therefore have led to a decrease in overall neural activity and in temporal coding precision. However, previous studies have shown that neural responses measured in bats anesthetized with medetomidine, midazolam, and fentanyl reflected the behavioral performance of the bats well (Firzlaff et al. 2006, 2007). The influence of the anesthesia should therefore only be moderate.

Coding of Communication Calls in Relation to SAM Stimuli

The dorsal AC is also an important area in terms of the processing of species-specific communication sounds in bats. The delay-tuning properties of units in the AC of the mustached bat seem also to facilitate the responses to combination of syllables of communication calls (Esser et al. 1997; Ohle-

miller et al. 1996), therefore serving processing of syntax in bat vocal communication. Interestingly, nonlinear temporal and spectral integration appear to underlie processing of communication sounds in other mammals, thus representing a general principle in vocal communication (Kanwal and Rauschecker 2007).

Selectivity indexes of the recorded units in our study (mean d_i value 0.3153) were similar to values reported for the marmoset A1 (mean d_i values between 0.335 and 0.479; Wang and Kadia 2001) but substantially higher than the cat A1 (mean d_i values between 0.047 and 0.086; Wang and Kadia 2001). Wang and colleagues (Wang et al. 1995; Wang 2000) described aforementioned call selectivity in marmoset A1 units, and they hypothesized a specialization in fast and precise detection of frequently heard vocalizations, which also seems applicable to the units in the AC of *P. discolor*. Additionally, we found that the temporal envelope-coding properties of units often correlated with a preference for aggression calls (showing strong amplitude modulations around 130 Hz) expressed by neuronal firing rate as well as in spike timing patterns reflecting the temporal call envelope. Quite similar findings were reported for the primary AC of anesthetized marmosets, where responses to twitter calls correlated with responses to SAM sounds with comparable modulation rates (Nagarajan et al. 2002) and responses of units were phase-locked to parts of the envelope of communications calls (Wang et al. 1995). Whether this response correlation to sound envelope is enough to create a call-specific representation in single units or is used to synchronize a larger neuronal population, i.e., to create a population code for vocalizations (Wang et al. 1995), is still not clear for the dorsal AC in *P. discolor* and has to be investigated in future experiments.

The fact that response PSTH spectra often showed peaks in the 100- to 130-Hz range, reflecting peaks in the call envelope spectra, does not mean, per se, that the complete call envelope is thoroughly encoded in the response pattern. For SAM stimuli, phase-locking to higher modulation frequencies of did not occur over the full range of modulation cycles, i.e., not over the complete stimulus duration (e.g., Fig. 4). In addition, strong overall fluctuations of call intensity superimposed on faster envelope modulation might impair the neural response when becoming subthreshold. We therefore can only demonstrate the principle ability of *P. discolor* neurons to respond to high-frequency modulations in the call envelope of communication calls in this study, but we cannot demonstrate high-fidelity coding of the complete call envelope that might be necessary for response specificity to individual calls.

In conclusion, our results show that units in the dorsal AC of the bat *P. discolor* can encode fast temporal envelope modulations as both rate and temporal code. This ability is partly reflected in the neuronal response preference to certain types of species-specific communication calls characterized by temporal envelope modulations in the same frequency range. Therefore, neural processing in the dorsal AC of bats seems to be specifically adapted to the high envelope modulation rates occurring in the vocal repertoire and might therefore play an important role in vocal communication.

ACKNOWLEDGMENTS

We thank Lutz Wiegrebe for providing the experimental animals and Wolfgang Greiter for comments and input into the analysis.

GRANTS

This work was supported by Human Frontier Science Program Grant RGP0058 (to U. Firzlaff).

DISCLOSURES

No conflicts of interest, financial or otherwise, are declared by the authors.

AUTHOR CONTRIBUTIONS

S.G.H. and U.F. conceived and designed research; S.G.H. performed experiments; S.G.H. and U.F. analyzed data; S.G.H. and U.F. interpreted results of experiments; S.G.H. prepared figures; S.G.H. drafted manuscript; S.G.H. and U.F. edited and revised manuscript; U.F. approved final version of manuscript.

REFERENCES

Aguilar LA, Malmierca MS, Coveñas R, López-Poveda EA, Tramu G, Merchán M. Immunocytochemical distribution of Met-enkephalin-Arg6-Gly7-Leu8 (Met-8) in the auditory system of the rat. *Hear Res* 187: 111–121, 2004. doi:10.1016/S0378-5955(03)00333-2.

Andoni S, Li N, Pollak GD. Spectrotemporal receptive fields in the inferior colliculus revealing selectivity for spectral motion in conspecific vocalizations. *J Neurosci* 27: 4882–4893, 2007. doi:10.1523/JNEUROSCI.4342-06.2007.

Andoni S, Pollak GD. Selectivity for spectral motion as a neural computation for encoding natural communication signals in bat inferior colliculus. *J Neurosci* 31: 16529–16540, 2011. doi:10.1523/JNEUROSCI.1306-11.2011.

August PV. *Distress Calls in Artibeus jamaicensis: Ecology and Evolutionary Implications*, edited by Eisenberg JF. Washington, DC: Smithsonian Institution Press, 1979.

Bartenstein SK, Gerstenberg N, Vanderelst D, Peremans H, Firzlaff U. Echo-acoustic flow dynamically modifies the cortical map of target range in bats. *Nat Commun* 5: 4668, 2014. doi:10.1038/ncomms5668.

Bendor D, Wang X. Neural response properties of primary, rostral, and rostrotemporal core fields in the auditory cortex of marmoset monkeys. *J Neurophysiol* 100: 888–906, 2008. doi:10.1152/jn.00884.2007.

Bieser A, Müller-Preuss P. Auditory responsive cortex in the squirrel monkey: neural responses to amplitude-modulated sounds. *Exp Brain Res* 108: 273–284, 1996. doi:10.1007/BF00228100.

Bohn KM, Schmidt-French B, Ma ST, Pollak GD. Syllable acoustics, temporal patterns, and call composition vary with behavioral context in Mexican free-tailed bats. *J Acoust Soc Am* 124: 1838–1848, 2008. doi:10.1121/1.2953314.

Burger RM, Pollak GD. Analysis of the role of inhibition in shaping responses to sinusoidally amplitude-modulated signals in the inferior colliculus. *J Neurophysiol* 80: 1686–1701, 1998. doi:10.1152/jn.1998.80.4.1686.

Bürki C, Felix D, Ehrenberger K. Enkephalin suppresses afferent cochlear neurotransmission. *ORL J Otorhinolaryngol Relat Spec* 55: 3–6, 1993. doi:10.1159/000276344.

Buunen TJ, Rhode WS. Responses of fibers in the cat's auditory nerve to the cubic difference tone. *J Acoust Soc Am* 64: 772–781, 1978. doi:10.1121/1.382042.

Cohen YE, Theunissen F, Russ BE, Gill P. Acoustic features of rhesus vocalizations and their representation in the ventrolateral prefrontal cortex. *J Neurophysiol* 97: 1470–1484, 2007. doi:10.1152/jn.00769.2006.

Condon CJ, Galazyuk A, White KR, Feng AS. Neurons in the auditory cortex of the little brown bat exhibit selectivity for complex amplitude-modulated signals that mimic echoes from fluttering insects. *Aud Neurosci* 3: 269–287, 1997.

Covey E. Neurobiological specializations in echolocating bats. *Anat Rec A Discov Mol Cell Evol Biol* 287: 1103–1116, 2005. doi:10.1002/ar.a.20254.

Covey E, Carolina DN, Hawkins HL, Port RF (Editors). *Neural Representation of Temporal Patterns*. New York: Springer, 1995. doi:10.1007/978-1-4615-1919-5.

Creutzfeldt O, Hellweg FC, Schreiner C. Thalamocortical transformation of responses to complex auditory stimuli. *Exp Brain Res* 39: 87–104, 1980. doi:10.1007/BF00237072.

DiMattina C, Wang X. Virtual vocalization stimuli for investigating neural representations of species-specific vocalizations. *J Neurophysiol* 95: 1244–1262, 2006. doi:10.1152/jn.00818.2005.

Eggermont JJ. How homogeneous is cat primary auditory cortex? Evidence from simultaneous single-unit recordings. *Aud Neurosci* 2: 79–96, 1996.

Eggermont JJ. Representation of spectral and temporal sound features in three cortical fields of the cat. Similarities outweigh differences. *J Neurophysiol* 80: 2743–2764, 1998. doi:10.1152/jn.1998.80.5.2743.

Eggermont JJ. Temporal modulation transfer functions in cat primary auditory cortex: separating stimulus effects from neural mechanisms. *J Neurophysiol* 87: 305–321, 2002. doi:10.1152/jn.00490.2001.

Ehrlich D, Casseday JH, Covey E. Neural tuning to sound duration in the inferior colliculus of the big brown bat, *Eptesicus fuscus*. *J Neurophysiol* 77: 2360–2372, 1997. doi:10.1152/jn.1997.77.5.2360.

Esser K-H, Condon CJ, Suga N, Kanwal JS. Syntax processing by auditory cortical neurons in the FM-FM area of the mustached bat *Pteronotus parnellii*. *Proc Natl Acad Sci USA* 94: 14019–14024, 1997. doi:10.1073/pnas.94.25.14019.

Esser KH, Schubert J. Vocal dialects in the lesser spear-nosed bat *Phyllostomus discolor*. *Naturwissenschaften* 85: 347–349, 1998. doi:10.1007/s001140050513.

Feng AS. Neural mechanisms of target ranging in FM bats: physiological evidence from bats and frogs. *J Comp Physiol A Neuroethol Sens Neural Behav Physiol* 197: 595–603, 2011. doi:10.1007/s00359-010-0533-5.

Fenton MB, Belwood JJ, Fullard JH, Kunz TH. Responses of *Myotis lucifugus* (Chiroptera: Vespertilionidae) to calls of conspecifics and to other sounds. *Can J Zool* 54: 1443–1448, 1976. doi:10.1139/z76-167.

Firzlaff U, Schörnich S, Hoffmann S, Schuller G, Wiegrebe L. A neural correlate of stochastic echo imaging. *J Neurosci* 26: 785–791, 2006. doi:10.1523/JNEUROSCI.3478-05.2006.

Firzlaff U, Schuchmann M, Grunwald JE, Schuller G, Wiegrebe L. Object-oriented echo perception and cortical representation in echolocating bats. *PLoS Biol* 5: e100, 2007. doi:10.1371/journal.pbio.0050100.

Gadziola MA, Grimsley JMS, Shanbhag SJ, Wenstrup JJ. A novel coding mechanism for social vocalizations in the lateral amygdala. *J Neurophysiol* 107: 1047–1057, 2012. doi:10.1152/jn.00422.2011.

Gadziola MA, Shanbhag SJ, Wenstrup JJ. Two distinct representations of social vocalizations in the basolateral amygdala. *J Neurophysiol* 115: 868–886, 2016. doi:10.1152/jn.00953.2015.

Gaese BH, Ostwald J. Temporal coding of amplitude and frequency modulation in the rat auditory cortex. *Eur J Neurosci* 7: 438–450, 1995. doi:10.1111/j.1460-9568.1995.tb00340.x.

Gaese BH, Ostwald J. Anesthesia changes frequency tuning of neurons in the rat primary auditory cortex. *J Neurophysiol* 86: 1062–1066, 2001. doi:10.1152/jn.2001.86.2.1062.

García-Rosales F, Beetz MJ, Cabral-Calderin Y, Kössl M, Hechavarria JC. Neuronal coding of multiscale temporal features in communication sequences within the bat auditory cortex. *Commun Biol* 1: 200, 2018a. doi:10.1038/s42003-018-0205-5.

García-Rosales F, Martin LM, Beetz MJ, Cabral-Calderin Y, Kössl M, Hechavarria JC. Low-frequency spike-field coherence is a fingerprint of periodicity coding in the auditory cortex. *iScience* 9: 47–62, 2018b. doi:10.1016/j.isci.2018.10.009.

Gaucher Q, Huetz C, Gourévitch B, Laudanski J, Occelli F, Edeline JM. How do auditory cortex neurons represent communication sounds? *Hear Res* 305: 102–112, 2013. doi:10.1016/j.heares.2013.03.011.

Goldberg JM, Brown PB. Response of binaural neurons of dog superior olivary complex to dichotic tonal stimuli: some physiological mechanisms of sound localization. *J Neurophysiol* 32: 613–636, 1969. doi:10.1152/jn.1969.32.4.613.

Greiter W, Firzlaff U. Echo-acoustic flow shapes object representation in spatially complex acoustic scenes. *J Neurophysiol* 117: 2113–2124, 2017. doi:10.1152/jn.00860.2016.

Grothe B. Interaction of excitation and inhibition in processing of pure tone and amplitude-modulated stimuli in the medial superior olive of the mustached bat. *J Neurophysiol* 71: 706–721, 1994. doi:10.1152/jn.1994.71.2.706.

Grothe B, Covey E, Casseday JH. Medial superior olive of the big brown bat: neuronal responses to pure tones, amplitude modulations, and pulse trains. *J Neurophysiol* 86: 2219–2230, 2001. doi:10.1152/jn.2001.86.5.2219.

Hagemann C, Esser K-H, Kössl M. Chronotopically organized target-distance map in the auditory cortex of the short-tailed fruit bat. *J Neurophysiol* 103: 322–333, 2010. doi:10.1152/jn.00595.2009.

Hartmann WM, Pumplin J. Noise power fluctuations and the masking of sine signals. *J Acoust Soc Am* 83: 2277–2289, 1988. doi:10.1121/1.396358.

Hechavarría JC, Beetz MJ, Macias S, Kössl M. Distress vocalization sequences broadcasted by bats carry redundant information. *J Comp Physiol A Neuroethol Sens Neural Behav Physiol* 202: 503–515, 2016. doi:10.1007/s00359-016-1099-7.

Hechavarría JC, Kössl M. Footprints of inhibition in the response of cortical delay-tuned neurons of bats. *J Neurophysiol* 111: 1703–1716, 2014. doi:10.1152/jn.00777.2013.

Hechavarría JC, Macías S, Vater M, Voss C, Mora EC, Kössl M. Blurry topography for precise target-distance computations in the auditory cortex of echolocating bats. *Nat Commun* 4: 2587, 2013. doi:10.1038/ncomms3587.

Heil P, Schulze H, Langner G. Ontogenetic development of periodicity coding in the inferior colliculus of the Mongolian gerbil. *Aud Neurosci* 1: 363–383, 1995.

Hewitt MJ, Meddis R. A computer model of amplitude-modulation sensitivity of single units in the inferior colliculus. *J Acoust Soc Am* 95: 2145–2159, 1994. doi:10.1121/1.408676.

Hoffmann S, Firzlaff U, Radtke-Schuller S, Schwellnus B, Schuller G. The auditory cortex of the bat *Phyllostomus discolor*: localization and organization of basic response properties. *BMC Neurosci* 9: 65, 2008. doi:10.1186/1471-2202-9-65.

Hoglen NEG, Larimer P, Phillips EA, Malone BJ, Hasenstaub AR. Amplitude modulation coding in awake mice and squirrel monkeys. *J Neurophysiol* 119: 1753–1766, 2018. doi:10.1152/jn.00101.2017.

Jen PHS, Hou T, Wu M. Neurons in the inferior colliculus, auditory cortex and pontine nuclei of the FM bat, *Eptesicus fucus* respond to pulse repetition rate differently. *Brain Res* 613: 152–155, 1993. doi:10.1016/0006-8993(93)90466-Z.

Joris PX, Schreiner CE, Rees A. Neural processing of amplitude-modulated sounds. *Physiol Rev* 84: 541–577, 2004. doi:10.1152/physrev.00029.2003.

Joris PX, Yin TC. Responses to amplitude-modulated tones in the auditory nerve of the cat. *J Acoust Soc Am* 91: 215–232, 1992. doi:10.1121/1.402757.

Kanwal JS, Ehret G. Communication sounds and their cortical representation. In: *The Auditory Cortex*, edited by Winer JA, Schreiner CE. Boston, MA: Springer, 2011, p. 343–367.

Kanwal JS, Matsumura S, Ohlemiller K, Suga N. Analysis of acoustic elements and syntax in communication sounds emitted by mustached bats. *J Acoust Soc Am* 96: 1229–1254, 1994. doi:10.1121/1.410273.

Kanwal JS, Rauschecker JP. Auditory cortex of bats and primates: managing species-specific calls for social communication. *Front Biosci* 12: 4621–4640, 2007. doi:10.2741/2413.

Köppl C. Phase locking to high frequencies in the auditory nerve and cochlear nucleus magnocellularis of the barn owl, *Tyto alba*. *J Neurosci* 17: 3312–3321, 1997. doi:10.1523/JNEUROSCI.17-09-03312.1997.

Krishna BS, Semple MN. Auditory temporal processing: responses to sinusoidally amplitude-modulated tones in the inferior colliculus. *J Neurophysiol* 84: 255–273, 2000. doi:10.1152/jn.2000.84.1.255.

Langner G. Periodicity coding in the auditory system. *Hear Res* 60: 115–142, 1992. doi:10.1016/0378-5955(92)90015-F.

Lu Y, Jen PH, Wu M. GABAergic disinhibition affects responses of bat inferior collicular neurons to temporally patterned sound pulses. *J Neurophysiol* 79: 2303–2315, 1998. doi:10.1152/jn.1998.79.5.2303.

Martin LM, García-Rosales F, Beetz MJ, Hechavarría JC. Processing of temporally patterned sounds in the auditory cortex of Seba's short-tailed bat, *Carollia perspicillata*. *Eur J Neurosci* 46: 2365–2379, 2017. doi:10.1111/ejn.13702.

Mittmann DH, Wenstrup JJ. Combination-sensitive neurons in the inferior colliculus. *Hear Res* 90: 185–191, 1995. doi:10.1016/0378-5955(95)00164-X.

Nagarajan SS, Cheung SW, Bedenbaugh P, Beitel RE, Schreiner CE, Merzenich MM. Representation of spectral and temporal envelope of twitter vocalizations in common marmoset primary auditory cortex. *J Neurophysiol* 87: 1723–1737, 2002. doi:10.1152/jn.00632.2001.

Naumann RT, Kanwal JS. Basolateral amygdala responds robustly to social calls: spiking characteristics of single unit activity. *J Neurophysiol* 105: 2389–2404, 2011. doi:10.1152/jn.00580.2010.

Nourski KV, Brugge JF. Representation of temporal sound features in the human auditory cortex. *Rev Neurosci* 22: 187–203, 2011. doi:10.1515/rns.2011.016.

O'Neill WE, Suga N. Target range-sensitive neurons in the auditory cortex of the mustache bat. *Science* 203: 69–73, 1979. doi:10.1126/science.758681.

Ohlemiller KK, Kanwal JS, Suga N. Facilitative responses to species-specific calls in cortical FM-FM neurons of the mustached bat. *Neuroreport* 7: 1749–1755, 1996. doi:10.1097/00001756-199607290-00011.

Olsen JF, Suga N. Combination-sensitive neurons in the medial geniculate body of the mustached bat: encoding of target range information. *J Neurophysiol* 65: 1275–1296, 1991. doi:10.1152/jn.1991.65.6.1275.

Peterson DC, Wenstrup JJ. Selectivity and persistent firing responses to social vocalizations in the basolateral amygdala. *Neuroscience* 217: 154–171, 2012. doi:10.1016/j.neuroscience.2012.04.069.

Radtke-Schuller S, Schuller G, O'Neill WE. Thalamic projections to the auditory cortex in the rufous horseshoe bat (*Rhinolophus rouxi*). II. Dorsal fields. *Anat Embryol (Berl)* 209: 77–91, 2004. doi:10.1007/s00429-004-0425-y.

Rees A, Møller AR. Stimulus properties influencing the responses of inferior colliculus neurons to amplitude-modulated sounds. *Hear Res* 27: 129–143, 1987. doi:10.1016/0378-5955(87)90014-1.

Rhode WS, Greenberg S. Encoding of amplitude modulation in the cochlear nucleus of the cat. *J Neurophysiol* 71: 1797–1825, 1994. doi:10.1152/jn.1994.71.5.1797.

Robertson D, Mulders WHAM. Distribution and possible functional roles of some neuroactive peptides in the mammalian superior olivary complex. *Microsc Res Tech* 51: 307–317, 2000. doi:10.1002/1097-0029(20001115)51:4<307:AID-JEMT2>3.0.CO;2-4.

Russ JM, Jones G, Mackie IJ, Racey PA. Interspecific responses to distress calls in bats (Chiroptera: Vespertilionidae): A function for convergence in call design? *Anim Behav* 67: 1005–1014, 2004. doi:10.1016/j.anbehav.2003.09.003.

Sanchez JT, Gans D, Wenstrup JJ. Glycinergic "inhibition" mediates selective excitatory responses to combinations of sounds. *J Neurosci* 28: 80–90, 2008. doi:10.1523/JNEUROSCI.3572-07.2008.

Sayegh R, Casseday JH, Covey E, Faure PA. Monaural and binaural inhibition underlying duration-tuned neurons in the inferior colliculus. *J Neurosci* 34: 481–492, 2014. doi:10.1523/JNEUROSCI.3732-13.2014.

Schnupp JW, Hall TM, Kokelaar RF, Ahmed B. Plasticity of temporal pattern codes for vocalization stimuli in primary auditory cortex. *J Neurosci* 26: 4785–4795, 2006. doi:10.1523/JNEUROSCI.4330-05.2006.

Schreiner CE, Urbas JV. Representation of amplitude modulation in the auditory cortex of the cat. II. Comparison between cortical fields. *Hear Res* 32: 49–63, 1988. doi:10.1016/0378-5955(88)90146-3.

Schuller G, Radtke-Schuller S, Betz M. A stereotaxic method for small animals using experimentally determined reference profiles. *J Neurosci Methods* 18: 339–350, 1986. doi:10.1016/0165-0270(86)90022-1.

Schulze H, Langner G. Periodicity coding in the primary auditory cortex of the Mongolian gerbil (*Meriones unguiculatus*): two different coding strategies for pitch and rhythm? *J Comp Physiol A Neuroethol Sens Neural Behav Physiol* 181: 651–663, 1997. doi:10.1007/s003590050147.

Schwartz C, Tressler J, Keller H, Vanzant M, Ezell S, Smotherman M. The tiny difference between foraging and communication buzzes uttered by the Mexican free-tailed bat, *Tadarida brasiliensis*. *J Comp Physiol A Neuroethol Sens Neural Behav Physiol* 193: 853–863, 2007. doi:10.1007/s00359-007-0237-7.

Sullivan WE 3rd. Neural representation of target distance in auditory cortex of the echolocating bat *Myotis lucifugus*. *J Neurophysiol* 48: 1011–1032, 1982. doi:10.1152/jn.1982.48.4.1011.

Ter-Mikaelian M, Sanes DH, Semple MN. Transformation of temporal properties between auditory midbrain and cortex in the awake Mongolian gerbil. *J Neurosci* 27: 6091–6102, 2007. doi:10.1523/JNEUROSCI.4848-06.2007.

Wang X. On cortical coding of vocal communication sounds in primates. *Proc Natl Acad Sci USA* 97: 11843–11849, 2000. doi:10.1073/pnas.97.22.11843.

Wang X, Kadia SC. Differential representation of species-specific primate vocalizations in the auditory cortices of marmoset and cat. *J Neurophysiol* 86: 2616–2620, 2001. doi:10.1152/jn.2001.86.5.2616.

Wang X, Merzenich MM, Beitel R, Schreiner CE. Representation of a species-specific vocalization in the primary auditory cortex of the common marmoset: temporal and spectral characteristics. *J Neurophysiol* 74: 2685–2706, 1995. doi:10.1152/jn.1995.74.6.2685.

Washington SD, Kanwal JS. DSCF neurons within the primary auditory cortex of the mustached bat process frequency modulations present within social calls. *J Neurophysiol* 100: 3285–3304, 2008. doi:10.1152/jn.90442.2008.

Washington SD, Kanwal JS. Sex-dependent hemispheric asymmetries for processing frequency-modulated sounds in the primary auditory cortex of the mustached bat. *J Neurophysiol* 108: 1548–1566, 2012. doi:10.1152/jn.00952.2011.

Whitfield IC, Evans EF. Responses of auditory cortical neurons to stimuli of changing frequency. *J Neurophysiol* 28: 655–672, 1965. doi:10.1152/jn.1965.28.4.655.